
Introduction and Literature Review

- 1.1. Introduction**
- 1.2. Overview of HPM System**
 - 1.2.1. Prime Power Supply**
 - 1.2.2. Pulse Power Supply**
 - 1.2.3. HPM Sources**
 - 1.2.4. Mode Convertor**
 - 1.2.5. Antenna**
- 1.3. Narrowband HPM Sources**
 - 1.3.1. Present Status of HPM Devices**
- 1.4. Different Types of HPM Devices**
 - 1.4.1. Relativistic Magnetron**
 - 1.4.2. Relativistic Backward Wave Oscillator**
 - 1.4.3. Relativistic Klystron**
 - 1.4.4. Free Electron Laser**
 - 1.4.5. Relativistic Gyrotron Devices**
 - 1.4.6. Virtual Cathode Oscillator**
- 1.5. Magnetically Insulated Line Oscillator (MILO)**
 - 1.5.1. MILO Components**
 - 1.5.2. Principle of Operation**
 - 1.5.3. Principle of Self Magnetic Insulation**
- 1.6. Literature Review of MILO**
- 1.7. Motivation and Objective**
- 1.8. Plan and Scope**

1.1. Introduction

In recent years, application of high power microwaves (HPM) for civilian and military, has led to the determined efforts on R&D interest of the HPM devices. These include the improvement of conventional devices and also the development of new HPM devices in the microwave and millimetre-wave ranges. It is intended to be used to intentionally disturb or destroy electronic equipments without damaging the infrastructure or hurting people. The expected outcome of an HPM attack can be a hard kill, where the electrical components are physically damaged, or a soft kill, where the components are disabled with malfunction as a result. In general, the power coupled into an object depends on the area sensitive to radiation, the coupling cross section. For front door coupling this is often the area of a slot or the aperture area of an antenna. If the frequency of the HPM pulse is within the bandwidth of the antenna, more energy is coupled in but the effect falls off rapidly for other frequencies. For back door coupling it is more complicated and the cross section depends on both frequency and position. The optimal coupling frequency for an object is hardly ever known beforehand. There are two main approaches to use HPM: one is to use a narrow band source, where the radiated energy is concentrated in a small frequency band. Another one is to use a wide band source, where the energy is radiated over a large frequency band as shown in Fig. 1.1. The upper figures show the pulse in time domain and the lower one in the frequency domain.

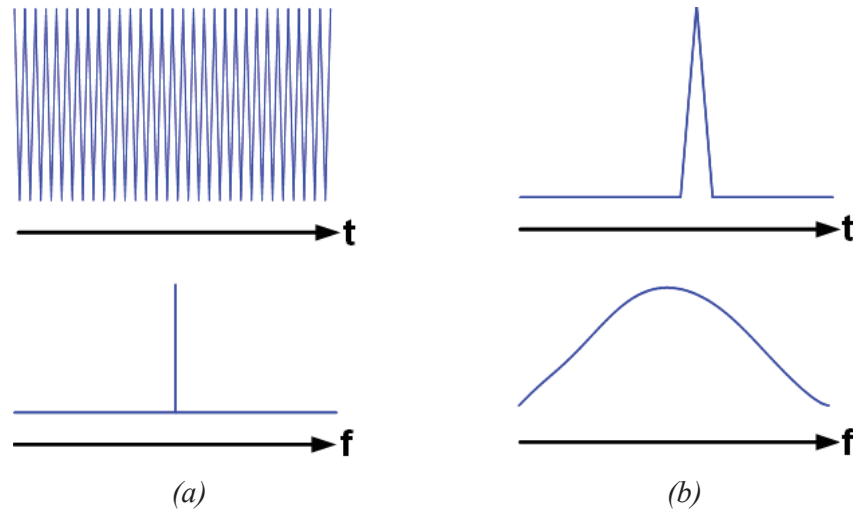


Fig. 1.1: Different types of HPM pulses: The upper figures show the time domain and the lower the frequency domain. (a) Narrow band and (b) Wide band.

With a wide band source, the chances are good that some energy is coupled in at a frequency where the object is sensitive, but the energy is small and the effects are also small. If a narrow band source is tuned to a frequency at which the target is sensitive, the effects can be large, but it is difficult to know what frequency will give the best coupling. A narrow band source that is tunable in frequency can cover a larger frequency band with several HPM pulses with different frequencies. For short pulses, less than 100 ns, thermal diffusion can be neglected and the power needed to damage a semiconductor component by a hard kill varies as t^{-1} . For longer pulses, between 100 ns and 1 μ s, energy is transported away by thermal diffusion and the power needed varies with $t^{-1/2}$. To damage electronics with a short pulse, a little energy but a high power is needed, whereas high energy and lower power is needed with a longer pulse. Another way to enhance the effect of HPM is to use repetitive pulses. To obtain thermal stacking, where the energy has no time to diffuse between the pulses, a pulse repetition rate of more than 1 kHz is needed. It is however likely that much lower repetition rate

will have effect since each pulse can degrade the material, with a lower threshold for damage than originally as a result. The radiated power is depending on the physical size of the HPM system. Both the radiation source and the power supply get larger with power. Therefore the more powerful systems with radiated powers over 1 GW are best suited for stationary installations, e.g. on a war ship or on a site. When there are no limitations in space, large antennas can be used to focus the radiated beam. Smaller systems with an output power of less than 1 GW can be mounted on vehicles, like a truck, or be used as HPM warheads in missiles.

1.2. Overview of HPM System



Fig. 1.2: Block diagram of an HPM system.

The general block diagram of an HPM system is shown in Fig. 1.2. This includes the following major sub-systems are: Power supply, pulse power generator, high power microwave source, and a radiator (antenna).

1.2.1. Prime Power Supply

Prime power supply that generates low power electrical input in a long pulse or continuous mode. For linking the prime power to the pulse power supply, the important parameters are the average power, repetition rate which together define the energy per pulse and the output voltage. There are many technological choices for prime power. One option is to employ a continuous prime power output to a number of pulse power options which would ultimately drive the HPM source. A common choice of primary power supply is to use a generator powered by internal combustion engine such as

diesel generator or the turbo generator, but it is also possible to drive pulse power supply with batteries for long periods. In either case the common feature of the sub-systems options is that either an alternating current (AC) internal combustion generator or a direct current (DC) battery provides long-pulse or continuous power that is converted to a DC output that functions as input to the pulse power supply.

1.2.2 Pulse Power Supply

In general, HPM sources need drivers that can supply short, intense electrical pulses of 1MV or more for upto 1 μ s duration. This can be achieved by pulse compression or by using capacitor banks that can transform a low voltage, slowly rising signal into a high-voltage, fast rising signal. However, one must ensure that the driver delivers a well-matched signal with regards to voltage and impedance. The conventional microwave sources typically operate on relatively low voltage and high impedance, but the HPM sources require substantially higher voltage levels and quite different impedance levels. This has been illustrated in Fig. 1.3. A mismatch between the impedance of the driver signal and the HPM source will result in poor energy transfer to the HPM source. This is particularly true if the impedance of the source is lower than the impedance of the driver. The choice of power supply and driver section will therefore largely be by the type of source to be used.

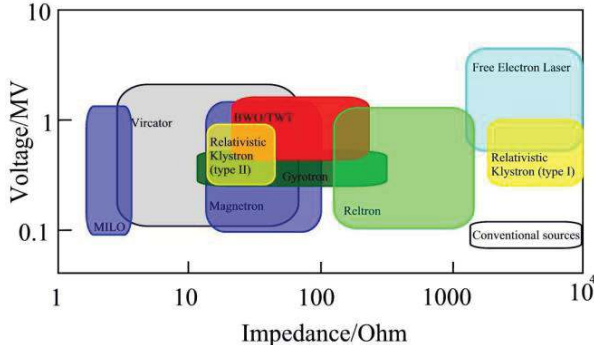


Fig. 1.3: Comparison of HPM sources and conventional microwave sources with respect to optimal impedance and voltage [Benford *et al.* (1991)].

A common configuration that consists of a Marx bank in which a row of capacitors are charged in parallel and then later quickly switched into a series circuit, allowing the voltage to be multiplied by the number of capacitive stages in the Marx. This can serve as an initial current generator for a flux compression generator (FCG). In an FCG a magnetic coil is compressed either by explosive or magnetic forces so that the current level rapidly increases. Another common option is to replace the FCG by a Pulse Forming Line (PFL). A third option is the Swedish vircator [Elfsberg *et al.* (2004)], which directly generates the electrical pulse for the HPM source from a large Marx generator (20-steps Marx generator in the case of the Swedish vircator) charged through a charging aggregate.

1.2.3. HPM Sources

The basic process behind all vacuum electron beam sources is the conversion of kinetic energy in an electron beam into electromagnetic radiation. This conversion is made possible through resonant interactions between the Eigenmodes of cavities and/or waveguides and the natural oscillation modes in electron plasma. Sources are divided into slow-wave and fast-wave type devices, where the Eigenmodes of the waveguide have phase velocities that are either smaller or larger, respectively, than the speed of the light. In case of slow-wave devices, the Cerenkov radiation is produced when the electrons move faster than the phase velocity of the electromagnetic waves. In the latter case, the radiation is generated by having electrons pass either from one medium to another, where the two media have different refraction index, or through perturbations in the medium such as a grid or a perforated plate. As an alternative strategy, the radiation sources are categorized into three: Linear beam (O-type), cross field (M-type), and space charge type. In the first case, electrons move parallel to a strong magnetic field. In the second case, one utilizes the fact that charged particles will experience a

drift normal to E and B when these two fields are not parallel. The last case is based on the formation of so-called virtual cathodes when the current exceeds the space-charge limit. An external magnetic field is not strictly necessary in this case.

1.2.4. Mode Convertor

Mode convertor is used for tailoring the spatial distribution of electromagnetic energy to optimize the transmission of RF power and coupling to an antenna. High Power Microwave (HPM) sources, such as Relativistic Backward-Wave Oscillator (BWO), the gyrotron, and the Vircator (virtual cathode oscillator), generate RF power in cylindrically symmetric transverse electric TE_{0n} or transverse magnetic TM_{0n} modes. In particular TM_{01} mode is widely used in all HPM generation devices due to high power capacity and easy realization. However from the view point of antennas for high power, TM_{01} mode gives rise to doughnut configuration for a radiated pattern of the main lobe on the centre of E- and H-planes. The side lobe generation, gain reduction, and inefficient power loading on the antenna aperture, makes these modes unsuitable for driving conventional antennas. This gave an idea of using mode converters at the output of these sources to convert these modes into a plane-parallel linearly polarized beam. Vlasov antenna is one of the most known mode converters used. Thus for more effective illumination of microwave energy, antenna needs TE_{11} mode of circular waveguide which provides an easily optimized radiation pattern where major lobe contains maximum RF power and side lobes carry very less power. Therefore mode convertor is required between HPM source and antenna.

1.2.5. Antenna

The microwave radiator, like, antenna acts as the interface between the HPM source and the rest of the space. Antenna that radiates microwave electromagnetic energy output coming out of the mode convertor and compressing the output spatially

into a tighter and high intensity beam. An HPM source represents a challenge to conventional antenna technology due to the high levels of power and the short pulse lengths. The most important properties of an antenna are how well signals can be restricted to propagate in a specific direction and how effective the coupling between the antenna and the surrounding space is. The shape of the antenna can influence to what extent the phenomena known as air or dielectric breakdown is an issue or not while operating at high power levels. This phenomenon occurs if the local E-field is sufficiently strong. More specifically, the E-field needs to transfer enough energy to the electrons so that the atoms in the air become ionized after collisions with the high-energy electrons. At the atmospheric pressure level, this occurs at critical field strength of ~ 24 kV /cm. For pulses with a duration of more than 100 ns, ionospheric “plasma mirrors” can be formed at high altitudes which reflect relatively low-frequency microwaves (1GHz). The most common type of antennas for HPM sources are rectangular horn antenna. Recently, antenna arrays have presented themselves as promising alternatives.

1.3. Narrowband HPM Sources

To generate microwave powers over 100 MW, vacuum based electron-beam devices are preferred that convert the kinetic energy in an electron beam into microwave radiation [Benford *et al.* (2007)], [Barker *et al.* (2001)], [Hoad *et al.* (2004)], [Gold *et al.* (1997)]. The source is driven by a voltage pulse with amplitude of about 100 kV - 1 MV and a pulse length of about $1\mu\text{s}$. The operating frequency is some GHz and quite narrow banded, due to the nature of the source. There is an impressive increase in the output power of the conventional electron beam sources in the last few decades by the use of high density relativistic electron beam. The conventional slow wave high power sources based on relativistic effects include the relativistic magnetron, relativistic

klystron, relativistic BWO, etc. The fast wave devices capable of generating high power are the gyrotron, free electron laser, etc. Vircator is a popular simple and compact space charge HPM device that has very low overall efficiency due to mode competition and increased beam temperature which in turn reduces the beam bunching. In the magnetron, a voltage is applied between the inner cathode and the outer anode. Electrons are emitted from the cylindrical cathode, and due to the radial electric field and an external axial magnetic field, the electrons circle around the cathode. The radiation is often extracted from one vane in the anode. At the gaps of the cavities the electrons slow down and electron spokes are formed. The kinetic energy of the electron beam is transformed into the electromagnetic radiation. The frequency of the radiation is determined by the cavities resonant frequencies and it is hard to tune a magnetron in frequency during operation. It is very stable in frequency though and can generate high powers of several gigawatt. The difference between an ordinary magnetron and an HPM magnetron is the higher voltages and currents, which requires other electrode materials. The MILO (Magnetically Insulated Line Oscillator) is basically a linear magnetron [Clark *et al.* (1988)]. The major difference compared to an ordinary cylindrical magnetron is that the MILO does not require an external magnetic field. The current itself generates an axial magnetic field that prevents the electrons to short-circuit the anode-cathode gap. To generate the self insulating magnetic field an applied voltage of > 500 kV is needed. Since much of the energy goes to the magnetic field the MILO has lower efficiency than the magnetron. In a reltron an electron beam travels through a cavity where the beam bunches. The bunched beam is then accelerated in a gap with a high applied voltage, to a velocity close to the speed of light [Miller *et al.* (1992)]. The relativistic speed freezes the bunching and the velocity spread of the electrons is low,

with monochromatic radiation as a result. The microwave radiation is extracted in one or several cavities.

1.3.1 Present Status of HPM Devices

Microwave sources are operating in both the high-peak power (short pulse and low repetition rate) and high average power (long repetition rate or continuous-wave) regimes, even though the instantaneous power in two regimes are quite different. Moreover, high power for broadband amplifiers can be very different than high power for long pulse oscillator. A high-power microwave tube must incorporate a variety of technologies, including a high-power electron gun, a high-power RF circuit, a suitable RF vacuum window, and an electron-beam collector [Gold (1997)].

In 1930, several investigators realized that higher frequencies could be obtained using resonant cavities connected to the electrical circuits. The first cavity device, klystron was produced in 1937. After that according to need there were generated several devices like Magnetron, TWT and BWO in which some devices were O-Type and other M-Type. In 1960's crossed field amplifier was developed. The 1970's saw the strong emergence of solid state based microwave sources and then high power microwave devices has been thought to invent. HPM is generated at the expense of the electron beam kinetic energy. The driving electron beam pulses range from 10's to 100's ns in duration. Description of any high power microwave devices begins with generation of electron beam in particular type of electron gun and power supply used to drive it. This used in repetitively pulse, high average power and single shot, high peak power devices and also used in breakdown and others pulse shortening.

One of the classic effects of electron beam is to generate coherent electromagnetic spectrum. The development of sources of radiation in the microwave portion of electromagnetic spectrum which extends from 300 MHz to 300 GHz began many years

ago. However, an impressive increase in the power and operating frequency of these sources has taken place in last few decades due to progress in a new branch of physics that can be called “Relativistic High-Frequency Electronics.” The term “relativistic” refer to first high electron beam with velocity close to speed of light which can have very high current densities and second to the appearance of new microwave sources based on specific relativistic effect. This relativistic effect may be important even at low voltages, when velocity of electron is smaller than the speed of light. Use of high currents and voltages in conjunction with conventional devices such as klystron and magnetron; the development of new devices concept that rely specifically on these very high currents such as vircators and the research into new fast wave devices such as gyrotrons and free electron lasers, that make direct use of relativistic effects, that extrapolate to higher power at shorter wavelengths than conventional devices. The technical progress of the microwave sources over last several decades have been described by Barker and Schamiloglu (Fig. 1.4) in terms of Pf^2 (power times frequency squared, also referred to as the *quality factor*) [Barker and Schamiloglu (2001)]. The relativistic devices are referred.

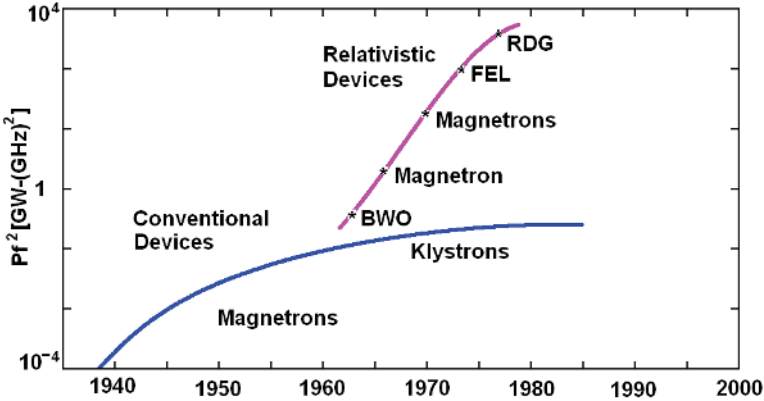


Fig. 1.4: Microwave devices Evolution: BWO (backward wave oscillator), FEL (free electron laser), and RDG (relativistic diffraction generator) [Barker and Schamiloglu (2001)].

for the HPM devices. Notice that though the output parameters from conventional devices have slowed considerably in recent decades, the HPM sources experienced significant increase in output power during the same period of time.

Basic use of pulsed power technology is to convert prime power sources into a short tailored high voltage pulse. Once pulse power portion of the system has produced the desirable high voltage waveform, it is applied to an electron gun which produces a high perveance electron beam where space-charge effects dominate the interaction. The relativistic electron beam, once generated propagates through RF interaction region, which converts the beam kinetic energy into HPM. It is the particular nature of this interaction that then distinguishes the various classes of sources [Chu (2004)], [Bratman *et al.* (1987)], [Gold and Nusinovich (1997)], [Caryotakis (1998)], [Gaponov and Granatstein (1994)].

HPM have both civilian and military applications that is divided based on the existing or potential applications of these sources are as 1) high-average power oscillators in resonance heating and current drive of thermonuclear fusion plasmas; 2) microwave and millimeter wave narrow band sources and amplifiers for RF acceleration in high-energy linear colliders; 3) broad band millimeter-wave amplifiers in radar and communication systems and 4) high-peak power sources for direct energy weaponry (DEW) of both the hard-kill type, which aims at the physical destruction of targets, and the soft-kill type, which makes the enemy's mission-critical components either inoperative or faulty. In this case, peak output powers on the order of 1 GW at frequencies on the order of 1 GHz in pulse durations as long as possible, but typically on the order of 100 ns are desirable. Repetitive pulse capability is also desirable, but becomes increasingly difficult at the highest output powers and longest pulse durations.

Apart from these the futuristic civilian applications of HPM include satellite power stations (SPS), artificially ionized layer (AIL) that addresses several problems like remote radio and TV communication, remote sensing of small components in the atmosphere, repair of the ozone hole, atmospheric purification of admixtures that destroy the ozone layer, etc.

1.4. Different Types of HPM devices

1.4.1. Relativistic Magnetron

The relativistic magnetron has been the most promising sources of HPM for many years. The fundamental difference between relativistic and conventional magnetrons is the application of much higher voltages and explosive emission cathodes.

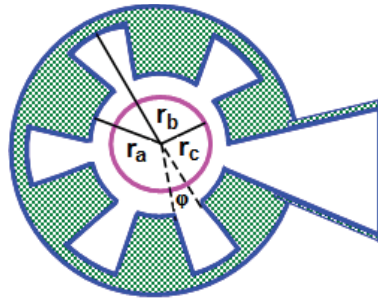


Fig. 1.5: Schematic of Relativistic Magnetron [Palevski *et al.* (1979)].

Table-1.1: Comparison of Conventional and Relativistic Magnetrons [Tsimring (2006)]

Parameter	Conventional Magnetron	Relativistic Magnetron
Maximum voltage	~ 10 kV	~ 1 MV
Maximum current	~ 100 A	~ 10 kA
Emission	Thermionic and secondary	Field emission
Maximum RF power	~ 10 MW	~ 1 GW
Maximum conversion efficiency	~ 85 %	~ 30 %
Pulse duration	> 1 μ s	< 100 ns
Maximum frequency	100 GHz	10 GHz

This allows one to overcome current limitations connected with cathode emission and space charge and to raise the current and output power by approximately two orders of magnitude. The relativistic magnetron was first developed in S-band with a six-sector cavity resonator, a graphite cathode, and a tapered output waveguide at the Massachusetts Institute of Technology (MIT), USA [by Bekefi *et al.* (1976)] as shown in Fig 1.5. It is operated at a 10-cm wavelength with a potential of 360 kV, a magnetic field 0.8 Tesla and a field emission current of 35 kA (without the magnetic field). This magnetron gave an output power of 1.7 GW with conversion efficiency of 35%, and pulse duration of 30 ns. This large pulse duration was essentially determined by the highly favorable diode orientation of the magnetic field in the magnetron for explosive emission, similar to magnetically insulated diodes. Average comparative parameters of conventional and relativistic magnetrons are given in Table 1.1 [Benford *et al.* 2007].

1.4.2. Relativistic Backward Wave Oscillator

Research activity in the generation of high-power microwave and millimeter-wave radiation has existed for about the last four decades. Many of the recent studies have been prompted by the availability of high-power, pulse line accelerators capable of producing intense, relativistic electron beams which drive the RF structures. One of the most successful examples of high-power microwave sources utilizing high-current relativistic electron beam is the backward-wave oscillator (BWO). The device consists of a periodic metallic structure inside which a high-current relativistic electron beam is injected as shown in Fig. 1.6 (a). A thin annular relativistic electron beam of radius r_b is generated by a cathode with explosive emission and propagates along strong axial magnetic field inside of a cavity with ripple walls. The length of the cavity is L , the average radius is r_{av} and the period is d . The wall radius is varying sinusoidally: $r_w(z) = r_{av} (1+h \sin(2\pi z/d))$, where $h = (r_{max}-r_{min})/r_{av}$. The beam is usually confined by a strong

axial magnetic field. The slow wave structure reduces the phase velocity of electromagnetic (EM) waves below the vacuum speed of light so that electrons in the relativistic electron beam can give up energy directly to one of the Eigenmodes of the structure. These devices are capable of producing coherent radiation in the centimeter- and millimeter-wavelength regimes at a power level of hundreds of megawatts with efficiency close to 40%. Continued research aimed at increasing radiation power in these devices led recently to the development of new sources such as the multi-wave Cerenkov generator (MWCG) and the relativistic diffraction generator (RDG), which reportedly produced 15 GW at 9.4 GHz and 2.8 GW at 47 GHz. Figure 1.6 (b) is the dispersion relation. The straight line which intersects the cold structure dispersion curve is the electron beam Doppler line, $\omega = kv_{z0}$, where v_{z0} is the beam initial velocity. The wave number k_- denotes the backward wave and k_+ denotes the forward wave, while the frequency for both waves is the same, ω .

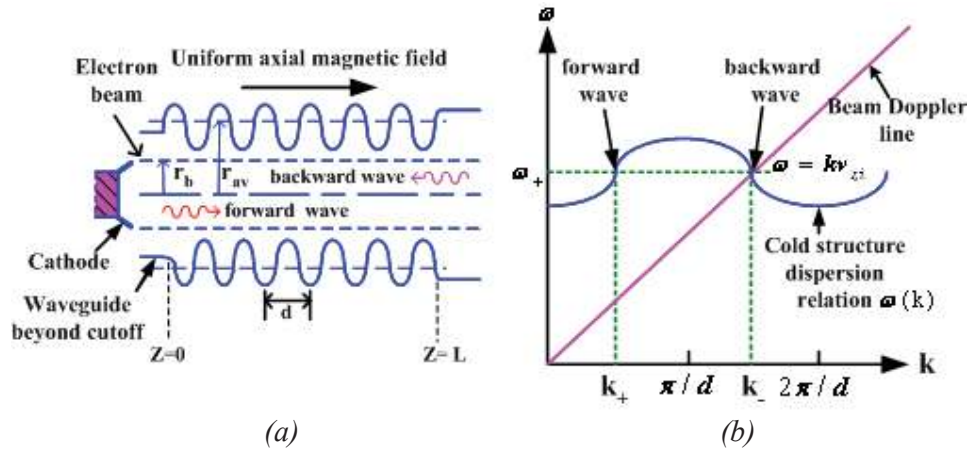


Fig.1.6: (a) Schematic of a Backward Wave Oscillator and (b) Dispersion characteristics of TM_{01} mode in an infinitely long periodic structure [Levush *et al.* (1992)].

1.4.3. Relativistic Klystron

The development of high power klystrons amplifiers with an enhanced voltage up to the relativistic electron energy was proposed primarily for charged particle accelerator

physics and in particular, RF linear accelerators (LINACs) for TeV electron colliders. A typical klystron amplifier consists of two or more cavities, separated by drift spaces, that are used to form electron bunches from an initially uniform electron flow by modulating the electron beam velocity using the axial electric fields of a transverse magnetic (*TM*) mode, followed by an output cavity that produces coherent radiation by decelerating the electron bunches. The schematic of relativistic klystron is shown in Fig. 1.7. The basic limitations on power as a function of frequency is determined by the output cavity, which must extract a significant fraction of the electron kinetic energy in a length limited by the electron transit time. The transit angle cannot exceed π in order to maintain a favorable RF phase in the cavity gap. Extracting the electron kinetic energy in a single RF gap becomes increasingly difficult both as the electron energy increases and as the frequency increases and multi-section cavity structures are required. The more complicated mode structure of these cavities often creates instability problems.

In general, three essentially different types of relativistic klystrons are known [Fazio *et al.* (1994)]. The first type is low-perveance klystrons with a solid beam, such as the pulse three-cavity relativistic klystron with voltage 400 kV developed at Stanford University in 1949 by the team of Chodorow and Ginzton [Chodorow *et al.* (1953)]. The operating frequency and the RF power of this klystron were as 3 GHz and 10 MW respectively. Advanced X-band SLAC klystrons of this type operate at voltage 1.3 MV, a current of 600 A, and produce 300 MW of power. The second type is relativistic multi-beam klystrons of a giga-watt power level (GMBK). The Stanford University designed a 10-beam L-band GMBK [Caryotakis *et al.* (1996, 1998)]. This GMBK should produce 1 GW with an efficiency of 40%. The beam voltage of this klystron is 500 kV, and the total current is 5.0 kA, so the current of the each beam is 500 A. The peculiarity of the GMBK is the use of the periodic permanent magnetic focusing. The

third type of relativistic klystrons is a high-current, high-perveance, mildly relativistic tube with an annular beam, generated by an explosive emission magnetically insulated diode, and coaxial cavities. These klystrons were investigated originally at the Naval Research Laboratory (NRL) [Friedman *et al.* (1990)]. The thin annular electron beam, propagating near a conducting wall of a large-diameter tube, can carry much higher currents than solid beams can. The typical value of the accelerating voltage is 500 kV, and the current of 5 to 20 kA is approximately an order of magnitude greater than the current in SLAC klystrons. The output power of the 1.3 GHz klystron was about 3 GW, the efficiency 50%, and the pulse duration up to 100 ns, with 37 dB gain [Lau *et al.* (1990)].

The basic use of relativistic klystrons is as high-energy drivers for electron and ion accelerators and colliders. An important use is in compact RF electron accelerators to drive free electron lasers and possible even high-frequency drivers for direct energy weapons [Barker and Schamiloglu, (2001)]. Increasing the radio frequency and pulse duration is a very important way to create multi-TeV linear colliders. Also, perspective radars and communication systems should operate at the W-band, where there is an atmospheric window. High-power efficiency relativistic klystrons do not exist at these frequencies because the dimensions of basic component became too small; frequencies of order 10 GHz are practically the upper boundary for these klystrons.

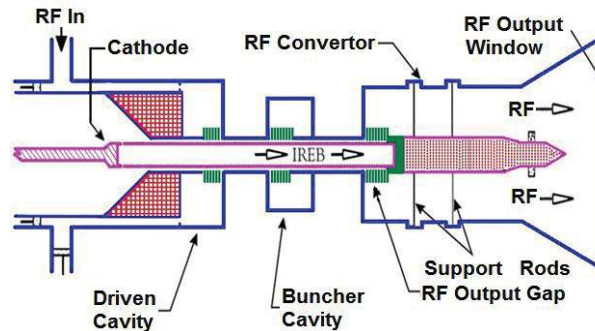


Fig. 1.7: Schematic of a Relativistic Klystron [Gold and Nusinovich, (1982)].

1.4.4. Free Electron Laser

Free-electron laser (FEL) is potentially the most flexible of all HPM sources, although they are also arguably the most complex. They offer almost unlimited frequency range, notwithstanding at the expense of increasingly high beam energies as the frequency goes up. In one remarkable series of experiments, an FEL was operated at repetition rates of over a kilohertz, with power levels of the order of a gigawatt at frequencies over 100 GHz. The original free-electron lasers (FELs) were referred as ubitrons which were developed in the 1950's. Like gyrotrons, free-electron lasers operate in the millimeter wave regime. The schematic of the FEL is shown in Fig. 1.8. The external force that causes transverse acceleration of the beam is typically alternating, transverse magnetic field lines known as the wiggler field. FEL beam quality requirements are similar to those of the gyrotron. Thus, they use high-quality relativistic beams as produced by accelerators. Linear accelerators, microtrons, and electrostatic accelerators have all been used in the low beam density, high beam voltage (Compton) operating regime. Induction accelerators are used in the high-beam density, lower voltage (Raman) regime [Granatstein and Alexeff, (1987)]. The FEL may be continuously tuned by changing the beam energy. Radiation in the far IR is produced by 1-2 MV beams. Beams of 10 to 1000 MeV produce radiation in the IR to UV range. Peak powers of greater than 1 GW have been reported. The intrinsic efficiency of a free-electron laser is very low. In the Compton regime it is a fraction of a percent; in the Raman regime it is a few percent. Tapered undulators (wigglers) produce reasonably with high efficiency ~ 40% has been reported.

The history of long-wavelength FEL research began with the thermionic Ubitron experiments of Phillips in the 1960's [Phillips (1960)]. In the 1970's, attempts were made to extend this work to high-peak-power levels using intense relativistic electron

beams from field emission diodes driven by pulse line accelerators. The efficiency of these early pulsed-power FEL experiments was typically $\ll 1\%$, due principally to the use of beams with excessively large velocity spreads, although an early experiment reported 30 MW at 10 GHz with $\sim 5\%$ efficiency from a FEL oscillator driven by a 700 kV electron beam [Marshall, (1985)], [Benford and Swegle, (1992)]. The breakthrough in efficiency in a millimeter-wave FEL came in an NRL experiment that used a beam-scraping diode to form a 1.35 MeV, 1.5 kA low emittance electron beam, and generated 35 MW at ~ 70 GHz with 2.5% efficiency [Parker *et al.* (1982)].

Because of their wavelength, coherence properties, tunability, intensity, and pulse duration, FELs demonstrate unprecedented capabilities for versatile applications across a variety of fields in science, technology, and industry. The span of possible applications of FELs is already considerable. Far from complete, the current list includes such areas as pharmacology, solid-state physics, chemistry and the chemical industries, civil engineering, shipbuilding, environmental sciences, defense, space-debris orbital control, polymer surface processing, micromachining, and the photophysics of complex polyatomic molecules. Especially interesting applications of FELs are in biology and biomedicine [Edwards *et al.* (2003)]. The latter include surgery, photo-dynamic therapy, and mammography. Important prospects have also been opened by the development of SASE FELs that can reach the hard x-ray range.

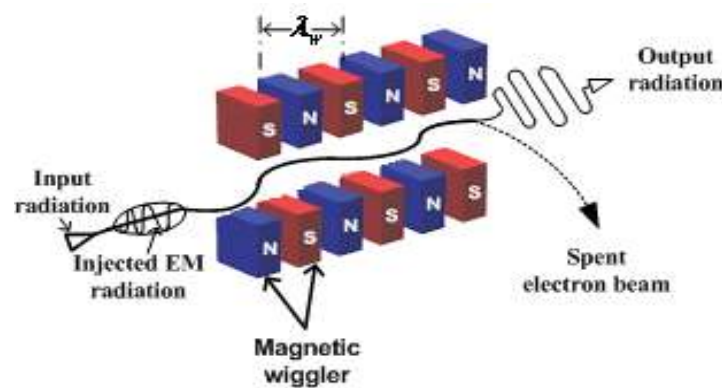


Fig. 1.8: Schematic of a FEL with planer wiggler

1.4.5. Relativistic Gyrotron Devices

Fast-wave gyro-devices are relative newcomers to the microwave tube family, also known as ‘electron cyclotron masers’, ‘cyclotron resonance masers’, or ‘gyrotrons’. Gyro-devices take advantage of a cyclotron resonance condition to transfer energy from an electron beam to an electromagnetic wave. The microwave frequency of the device and the magnitude of an applied DC magnetic field are intimately related by the synchronism condition. Fig.1.9 shows different types of gyrotron devices for their slow-wave and fast-wave (conventional). Gyrotrons are an extraordinarily mature source for high-average-power application at the several-megawatt level to the problem of heating magnetic fusion plasmas at electron cyclotron resonance frequencies of 100 GHz or more. Thermionic gyrotron oscillators have proved to be efficient sources of high-power microwave radiation and offer easy scaling to millimeter wave, and even to sub-millimeter wave frequencies.

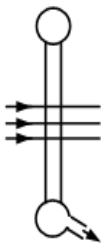
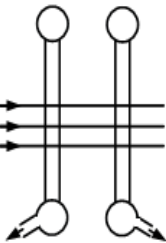
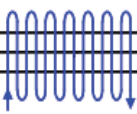
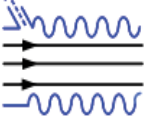
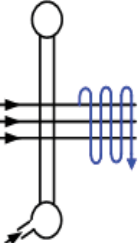
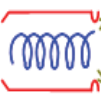
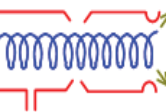
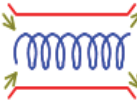
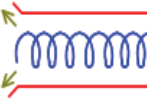
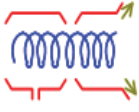
<p>Linear Beam Device</p>	 <p>Monotron</p>	 <p>Klystron</p>	 <p>TWT</p>	 <p>BWO</p>	 <p>Twystron</p>
<p>Type of Gyrotron</p>	 <p>Gyromonotron</p>	 <p>Gyroklystron</p>	 <p>Gyro-TWT</p>	 <p>Gyro-BWO</p>	 <p>Gyrotwystron</p>

Fig. 1.9: All types of Gyro devices [Gold and Nusinovich, (1982)].

This high-frequency advantage, compared to slow-wave devices, persists at higher voltage, even though the required magnetic fields scale upwards with the relativistic factor, γ . In fact, gyrotrons join klystrons as the only sources that are produced to continuously generate power levels at 1 MW or above. Another variant of this class of electron cyclotron masers, the gyro-klystron, has been investigated as an alternative to klystrons for power levels around 100 MW and frequencies in the X-band and above. Another variant, the *cyclotron auto-resonance maser* (CARM), potentially offers high power at high frequencies, since it features a linear up shift in frequency with beam energy, which compares to the quadratic frequency up shift of free-electron lasers without the complexity of wiggler magnets. In each case, however, these sources are immature at the giga-watt level, lacking the breadth and depth of development of other sources in comparable frequency ranges.

Studies of the gyrotron interaction using pulse line accelerators began in the 1970's. Among the initial studies was one using a 3.3MeV pulser to produce microwave peak powers of approximately 1 GW at 8 GHz; however, no resonant cavity was employed in that experiment, and the device produced microwaves with an efficiency of <1% [Granatstein *et al.* (1975)]. Subsequent studies employing resonant cavities were carried out primarily in the FSU, often employing 350keV, ~1kA electron beams. Among the results were 25MW at ~10GHz with 20% efficiency [Ginzburg *et al.* (1979)] and 23 MW at 40 GHz with 5% efficiency [Voronkov *et al.* (1982), Bogdanov *et al.* (1983)]. In addition, 60MW was produced at 15% efficiency in a plasma-filled gyrotron that operated above the vacuum space-charge limited current [Krementsov *et al.* (1978)]. Following this, a series of experiments was carried out at NRL between 1984 and 1989 that explored high-peak power gyrotron operation at 35 GHz and higher frequencies. In the NRL experiments, the beam transverse momentum was supplied by

sending the electron beam through a non-adiabatic dip in the magnetic field produced by a “kicker” magnet. A number of experiments were carried out at voltages of up to 800 kV and currents up to 1.6 kA using a compact Febetron pulser [Gold *et al.* (1987, 1988)]. These experiments produced 100 MW at 35 GHz with 8% efficiency in the TE₆₂ mode, and demonstrated high-power operation at frequencies ranging from 28 to 49 GHz by magnetically tuning through a family of TE_{*m*2} modes. The final experiment in this series operated on the much larger VEBA pulser at 1–1.35 MV and 2.5 kA, and produced 275 MW at 35 GHz in a 40-ns pulse with 14% efficiency [Black *et al.* (1990)]. Two decades ago, works on pulsed-power-driven gyro-devices, in particular the gyro-backward-wave oscillator (gyro-BWO) configuration has been carried out at the University of Michigan. Gyro-BWO producing 11 MW of RF power in the frequency range 3.2–6 GHz with a tapered axial magnetic field and operating at 700 – 900kV with a 1–4kA beam has been reported [Walter *et al.* (1996)]. NRL has explored gyro-klystron [Gold *et al.* (1990)] and gyro-traveling-wave amplifier configurations [Gold *et al.* (1991)] driven by pulse line accelerators. The latter experiment demonstrated 30 dB of gain at 35GHz, and produced 20MW at 11% efficiency in a circularly polarized TE₁₁ mode, using a 900keV, 300A low-velocity spread electron beam produced from an explosive-emission gun using a beam scraper as an emittance filter, and followed by a short bifilar helical wiggler magnet to produce the required transverse momentum. This gyro-TWA operated near “grazing intersection” between the dispersion curves for the beam and waveguide modes, where the upper (CARM) intersection and the lower (gyrotron) intersection merge, and could also have been considered a CARM amplifier, since the operating frequency was 4.4 times the relativistic cyclotron frequency. Menninger *et al.*, at MIT reported 4 MW at 17.1 GHz in a 20ns output pulse at 6.5% efficiency, with 51 dB of gain, from a gyro-TWT that

operated in the third cyclotron harmonic, using a 380keV, 160A electron beam from a thermionic electron gun driven by an induction accelerator [Menninger *et al.* (1996)].

Unlike the gyrotron, the frequency of the cyclotron auto-resonance maser (CARM) scales upwards in frequency as the voltage is increased, since the relativistic frequency up shift ($\sim \gamma^2$) more than cancels the relativistic decrease of the electron gyro-frequency (γ^{-1}), producing an overall γ scaling of the output frequency. However, like FELs and unlike gyrotrons, the presence of the Doppler term in the resonance condition makes CARM devices very sensitive to spreads in electron axial velocity (though they are insensitive to spreads in electron energy). Since the production of high-transverse momentum electron beams ($\beta_t \sim \gamma^{-1}$ is close to optimum) generally increases the axial velocity spread, CARM devices, both hot cathode and cold cathode, have generally fallen far short of their theoretical cold-beam efficiencies.

1.4.6. Virtual Cathode Oscillator (VIRCATOR)

Unlike the tubes discussed earlier, Virtual Cathode Oscillators (VCOs or Vircators) operate because of a phenomenon of intense beam physics. They have no conventional counterpart. Their general characteristics are operating frequencies in the range from 300 MHz to 40 GHz, simple construction, no magnetic field required (although they are sometimes used), broadband/tunable frequency, and very low efficiency [Schleher (1999), Hoerberling *et al.* (1992)]. It works on the principle of retarding an electron beam due to self-generated space charge force leading to the formation of a virtual cathode. The schematic of the vircator is as shown in Fig. 1.10. The Vircators consists of a field emitter type cathode and a mesh anode connected to a high voltage pulse power supply. The electron emitted by the cathode are accelerated by the mesh anode and injected in to the cylindrical drift space where there is no externally applied electric field. Beyond a critical value of the current density called the space charge limited

current, the electrons form a virtual cathode and repel the further electrons reaching them. The motion of electrons to and fro from the actual cathode to the virtual cathode lead to microwave radiations and the frequency will depend on the anode-cathode gap available. Operation is typically in a TM mode in a cylindrical geometry, making mode conversion necessary for efficient radiation. The frequency of oscillation of a free-running Vircators is related to the relativistic beam plasma frequency and typically chirps upward significantly during the pulse. Its frequency can be stabilized by employing a resonant cavity to contain the oscillating beam. If the resonant cavity is driven by an external source, the Vircators can be made to lock to the external signal. Phase locking and amplification at high powers with approximately 4.5 dB gain have been observed [Hoerberling *et al.* (1992)]. Although its simplicity is a major advantage, its very low efficiency is a real problem for reasonable weaponization. They have been used as a suite of sources for testing, where efficiency is not such an issue [Miner *et al.* (1992)]. Plasma closure effects limit pulse length and the ability to repetitively pulse—as is the case for most if not all HPM sources.

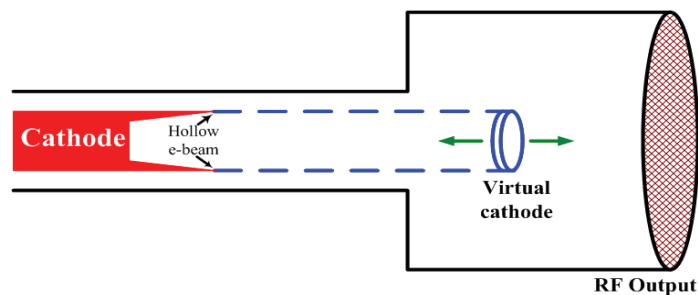


Fig. 1.10: Schematic of Virtual cathode Oscillator.

HPM sources like the vircator require high voltages and currents and the performance of the source depends highly on the electrode materials. Common emitter materials are velvet, carbon fiber or other materials with sharp tips. For dielectric materials like velvet, the electrons are emitted with explosive field emission, where the electrons are emitted from plasma that is formed around the fibers [Shiffler *et al.*

(2001), Adler *et al.* (1985), Miller *et al.* (1998)]. Too much plasma lowers the vacuum quality which in turn lowers the performance of the vircator. To reduce plasma formation a conducting emitter material like carbon velvet can be used [Shiffler *et al.* (2002), Garate *et al.* (1995), Roy *et al.* (2009)], where the electrons are emitted by field emission [Fowler *et al.* (1928)]. An applied electric field is enhanced at the tips and the electrons are allowed to tunnel directly from the material into vacuum. A vircator can be designed in different ways. Three most common geometries are the axial [Burkhart *et al.* (1987)] and coaxial vircators [Jiang *et al.* (1999)], and the reflex triode [Mahaffey *et al.* (1977)]. In the axial vircator and the reflex triode the anode and cathode are parallel and have the same center axis, while the anode and cathode of the coaxial vircator are cylinders sharing the same center axis. The reflex triode is positively pulsed on the inner conductor while the axial and coaxial vircators usually are negatively pulsed. To improve the performance of the vircator the virtual cathode can be enclosed in a resonance cavity [Benford *et al.* (1987)]. If the cavity is tuned to the operating frequency, higher fields can be extracted. Vircators tend to have a frequency chirp during the pulse but a resonance cavity can stabilize the frequency. In the axial vircator and the reflex triode the cavity can be a pillbox attached to the anode, enclosing the virtual cathode. The housing of the axial vircator is also a cavity defined by the vacuum tube. In the coaxial vircator, the cathode and anode act as cavities. In order to generate high powers a high current is needed and this requires a large emitting area. The coaxial vircator has the emitting area over the circumference of the cathode and therefore the axial width of the emitter can still be small. With narrower electron beam there can be a more defined excitation point for the generated microwave radiation.

Virtual cathode oscillators are enjoying something of a renaissance at this time, and developments with two variants in particular, tunable vircators and coaxial vircators,

may yet overcome two problems that have plagued devices of this type: low efficiency and sensitivity to gap closure in the high current, explosive emission diodes that are so often used with sources of this type. Nevertheless, despite their efficiency problems, these sources are attractive in applications requiring a simple source configuration — vircators many times employ no applied magnetic field and no slow-wave structure — and low device impedance, which permits high power operation at low voltage or optimizes coupling with low-impedance power sources such as explosive generators, which are a compact, energy-rich power source.

1.5. Magnetically Insulated Line Oscillator (MILO)

Magnetically insulated line oscillator (MILO) is a compact cross-field HPM source that differs from the magnetron primarily in that the insulating DC magnetic field, which together with the orthogonal DC electric field determines the electron drift, is generated by its own electron beam instead of the external magnetic field. This possibility requires such high current density that it can only be provided by an explosive electron emission. Consequently, MILO is an amazing combination of magnetic insulation, explosive emission, and interaction with retarding electromagnetic waves.

1.5.1. MILO Components

Fig. 1.11 shows the schematic of conventional MILO that comprises (i) cathode, (ii) slow wave structure (SWS) vanes, (iii) choke vanes or filter vanes, (iv) beam dump or collector, (v) extractor vane, and (vi) stub

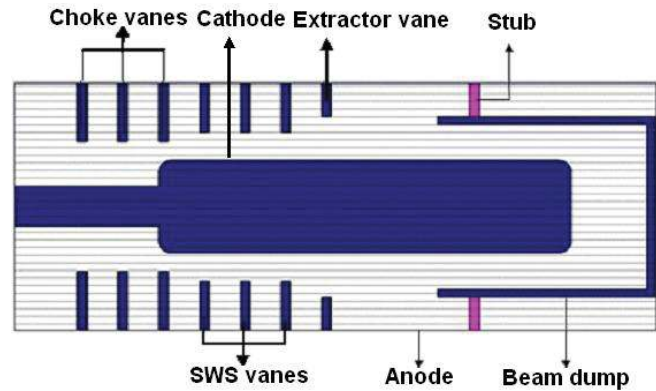


Fig. 1.11: Schematic of conventional MILO.

(i) Cathode

Peak power output and repetition mode operation of MILO depends on the cathode performance. The Pulse power source may deliver the required current however the cathode should be designed to provide the required emission current. An explosive emission cathode is used for Gigawatt-class sources of MILO. Because such cathodes “turn-on” at relatively low electric fields and deliver the very high-current densities of 100’s of A/cm² that allow the tube to generate extremely high RF power. On the other hand, these cathodes may introduce (undesirable) plasma downstream, causing electrical breakdown problems and may cause premature gap closure of the diode. Recent advances in the thermionic cathodes have pushed current densities above 10’ of A/cm² with reduced lifetime. Graphite /CsI coated or velvet cathode is used to achieve a high explosive emission. Either the emission portion of the cathode is fabricated using graphite or the stainless steel (SST) cathode is wrapped by velvet material pasted with metallic glue or SST coated with CsI. Mostly velvet is used for achieving very high field strength, subsequently to achieve very high emission current for single shot mode application. Recently Carbon fiber cathodes impregnated with cesium iodide salt (CsI) have proven to be a better choice than standard velvet cathodes. Because, the diode closure rate for the CsI carbon fiber cathode is less than 0.2 cm/μs, which is much less

than the typical $1.0 \text{ cm}/\mu\text{s}$ or greater. The velvet type cathode surface is preferred for distributed type emission because it maintains a high vacuum between 10^{-6} and 10^{-4} torr. When high voltage is applied a more matter is released in the inter electrode space, if the vacuum is not good. This is harmful for the device operation.

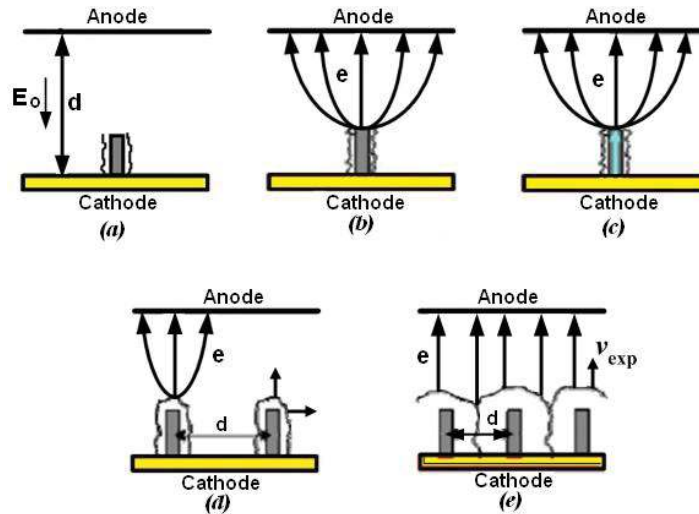


Fig. 1.12: Process of electron emission from a velvet surface. (a) The application of the intense electric field causes the partial destruction of fiber and the creation of a dense plasma column. (b) Electrons are emitted out of plasma and form a space charge current of the Child - Langmuir type. (c) Heating occurs in fiber due to Joules effect. (d) Expansion of the plasma column at the thermal speed. (e) Reduction of inter-electrode space by total expansion of the plasma of cathode.

The cold cathodes subjected to an intense electric field satisfy the law of the field emission. When electrons acquire a sufficient potential energy that is either by rise in temperature or due to application of intense electric field, they tear off and emitted in vacuum. This is accelerated by the potential difference between cathode and the anode. Fig. 1.12 shows the emission process of velvet cathode. Nowadays there are so many types of cathode are used, which has many advantages as compared to simple cathode. The dielectric fiber cathode which initiated surface flashover mechanism as the electric field exceeds $20 \text{ kV}/\text{cm}$. The other is carbon velvet field emitted cathode, which has been coated with a cesium iodide (CsI) salt. It has advantages including light weight and requires no heater for electron emission. In order to improve the pulse repetition

rate and the maintenance free lifetime of an improved MILO, new kind of metal dielectric cathode is being used. Explosive emission from the velvet is initiated by a surface flashover mechanism as the electric field exceeds 20 kV /cm. The surface discharge gives rise to a cold, dense plasma/gas column in nearly every fiber tufted on the velvet surface. The corresponding average material erosion rate for most velvet is 3×10^{15} mole /cm² that limits the velvet lifetime to $\sim 10^5$ pulses. The amount of the emitting centers and time delay in the electron emission depend strongly on the accelerating electric field growth rate. Carbon velvet cathodes coated with cesium iodide (CsI) has lifetime in excess of 980, 000 pulses with an out gassing rate of 3.5 atoms per electron.

(ii) Slow wave structure vanes

Outer cylinder of MILO consists of three circular discs that are periodically placed at a distance of L, which forms a periodic slow wave structure. This entire structure along with three SWS vanes acts as an anode of the MILO. It acts as an interaction structure where the RF signal interacts with electron beam. Number of discs adjusted according to power handling capacity and the width, period and depth of the SWS vane decides the operating frequency of the MILO. The TEM mode is generated inside the MILO structure; however extraction of RF power will be in TM₀₁ mode.

(iii) Choke or filter vanes

Choke vanes near the input side act as an in phase reflector or low pass filter. The first three discs are called as choke vanes. This is used to prevent the RF power in the main SWS structure from propagating upstream toward the pulse power system, and returning out of phase within the oscillating tube. The Microwave power that enters the RF choke region are completely reflected back into the primary SWS, which is critical for controlling the device performance. The RF choke is used to prevent radiation from

escaping the upstream end of the device by reflecting back into the interaction region. In addition, the impedance difference between the last choke disc and the first primary disc causes the electron flow in the primary SWS to move closer to the cavity openings where the RF voltage is strongest. This increases the power conversion efficiency. At lower impedance there is more current in the electron flow, and therefore, more power available for microwave generation.

Microwaves are generated in the MILO through an unstable interaction between slow electromagnetic modes and space-charge waves. A linear analysis of this microwave instability that includes the physics of magnetically insulated electron flow in the structure is totally verified. A tapered structure can adjust the group velocity of the generated wave at π -mode to propagate effectively. The numerical study for the efficient operation can be carried out using various 3-D computational codes such as MAGIC PIC code and CST Studio Suite.

(iv) Beam Dump/Collector

Beam dump act as a load that provides the return path for the flow of insulating current. The length of the cathode covered under beam dump region decides the operating current required for self-magnetic insulation as well as oscillation. The collector is made up of stainless steel (SS) or graphite (outer surface of the graphite to be covered by SS). Once the minimum required tailored length (L_{min}) of load is obtained, the actual length of the collector (L_{col}) can be calculated. It is necessary condition for the smooth functioning of MILO is $L_{col} \geq L_{Cmin}$. The collector–cathode space fixes the operating conditions of the diode. The recovery length of collector on cathode makes it possible to lengthen the duration of microwave pulse.

(v) Extractor Vane

The extractor vane plays a vital role in extracting the RF power out from MILO either radially through slots in resonators, or axially down the transmission line. The radial extraction is inefficient and yield only 1-2% efficiency, possibly because of disruption of π -mode. At the π -mode, the dispersion characteristics give zero group velocity that favors oscillations and limits the power flowing to the extraction cavity. In addition, a substantial fraction of the input energy used in the diode current which is needed to maintain the insulating azimuthal magnetic field in order to confine the beam between the anode and cathode region.

(vi) Stubs

Stubs at the output side will act as a short circuit for DC and open circuit for RF and also provides impedance matching at the output for maximum power conversion efficiency. It also acts as return path from beam dump to the anode so that the total anode current can self-generate the azimuthal magnetic field (B_θ) for creating insulation between the anode and cathode.

1.5.2. Principle of Operation

At high voltage electrons are emitted from the cathode but the current carried by the body (anode) creates a sufficiently strong magnetic field such that these electrons cannot cross the interaction gap. The electrons drift axially in the crossed electric and self-magnetic fields. A slow-wave structure is added to the anode so that the axially drifting electrons in the layer adjacent to the cathode interact with the axially directed slow electromagnetic wave to generate microwaves. Marx generator/Flux Compression Generator (FCG) is used to generate the required electrical pulse that initiates explosive electron emission in the cathode. The microwave oscillation is generated at the desired frequency and collected in extractor region of MILO. MILO is driven directly by either

Marx generator or Marx generator with pulse forming line. To achieve explosive emission in uniform rate, the rise time of the pulse should be less than 10 ns in order to avoid non-uniform emission at the cathode surface and it can be achieved by low impedance Marx generator with pulse forming line. The current delivered by the pulse power supply should be more than the critical current requirement of MILO. If the pulse power supply delivers required rise time and pulse width of MILO, then any variation in the shape of waveform above the envelope won't affect the MILO operation. Slow-wave structure design decides the frequency of the MILO and the operating frequency of the MILO is decided by the design of SWS. The extractor vane is used to extract the RF power and couple to the mode converter and the design of extractor vane decides the efficiency of the device. Collector/beam dump is used to provide the path for insulating current, which is used to converge the electrons to the cathode. The mode converter is introduced between MILO and antenna to convert from TM_{01} mode to TE_{11} mode. Necessary diagnostics are provided to measure the radiated RF power from the antenna. Initially MILO devices have been tested with 5% efficiency. With improved designs like tapered MILO, the efficiency has been enhanced to 20%. Figure 1.13 shows the strong spoke formation in the MILO.

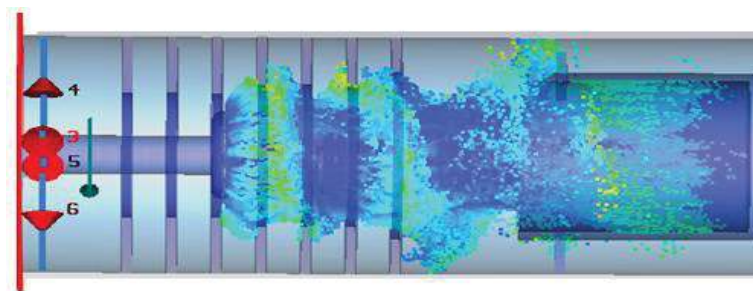


Fig. 1.13: Spoke formation in MILO

The RF power can be extracted from the MILO either radially through slots in resonators, or axially down the transmission line. The distance between the cathode and collector decides the magnetic cutoff, for the optimized operation of the device. A

MILO with three or more cavities oscillates readily in its fundamental π -mode. In this mode, each cavity in the slow wave structure behaves as a quarter-wave oscillator shifted in phase by approximately π from its neighbors. The quarter wave oscillations have maximum magnetic field at the cavity top, and maximum electric field to the electron flow in the MILO that develops a spoke-like structure as the electrons give up their potential to the electromagnetic field. Hence high power microwave is generated in TM_{01} mode at the desired frequency.

1.5.3. Principle of Self Magnetic Insulation

The magnetic insulation is created either by means of externally applied magnetic field or self-generated magnetic field that act perpendicular to the electric field in order to confine the electron beam. The anode (body) current should be more than the minimum critical current required by the geometry to create sustained self-magnetic insulation, as shown in Fig. 1.14. When the anode current is less than the critical current, all electrons emitted by the cathode reaching the anode causes electrical breakdown between A-K gap and no insulation occurs between anode and cathode.

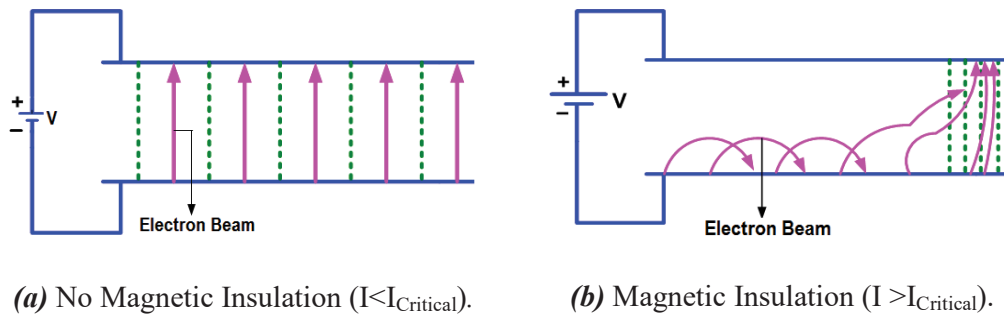


Fig. 1.14: Self- magnetic insulation mechanism.

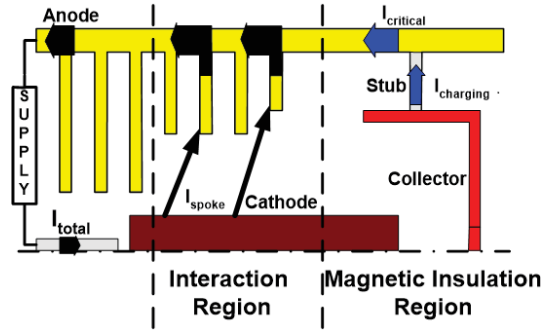


Fig .1.15: Schematic of current flow in MILO device.

When the anode current is more than critical current, all the electrons are confined between anode and cathode due to self-magnetic field generated by the anode current. This is the basic concept for producing very high-power microwave pulses in a device called MILO. Conditions of magnetic cut-off and interaction in the device are controlled by the load current. Further, the load current is decided by the space between collector and cathode. The space between the collector and cathode is optimized in order to allow a maximum current, in the slow wave structure, for better interaction. The following currents are defined in the MILO operation:

Charging current (I_{charging}): Initial current flowing from the cathode to collector, which decides the magnetic insulation

Critical current (I_{critical}): The minimum current needed to generate the self-magnetic field to create the insulation between the anode and cathode

Escape current or Spoke current (I_{spoke}): Current flowing from the cathode to slow wave structure vanes during the oscillation period called Escape current or Spoke current, which is responsible for generating the RF power

Parapotential current (I_p): The total current supported by the anode structure to sustain the self-magnetic insulation. This plays the significant role in providing the insulation between the cathode and anode

The anode current should not be too high compared to critical current, then tube will go into deep insulation and no RF power will be generated. Anode current should not be too lower than critical current, then beam will not reach collector. For the proper MILO operation, charging current neither is too low nor too high and it should be in synchronism with critical current.

1.6. Literature Review

In 1976 Bekefi *et al.*, suggested that the microwave emission is obtained from magnetically insulated relativistic electron-beam diodes in which magnetic fields could be self-generated within a cathode of a non-slow wave magnetically insulated microwave generator. During 1983, Mendel Jr. had proposed the theory of magnetically insulated transmission line (MITL) as the magnetic insulation is essential for the operation of large pulsed power systems. It is also reported that in the absence of magnetic insulation electrons will quickly short out the system if explosive emission occurs from the surface that is subjected to electric field greater than 2 kV/cm. Clark *et al.* in 1987 published the theory and simulation of high power microwave generation in Magnetically Insulated Line Oscillator (MILO). In this paper a dispersion relation is derived for cylindrical MILO using thin beam approximation. The dispersion relation is used to predict the frequency and growth rate of microwave generating instability.

In 1988, Clark *et al.*, reported a simulation on “Magnetically Insulated Line Oscillator(MILO)”, 1.5GHz with an efficiency 10%. They had discussed different geometries including planar, coaxial and concentric structure for MILO configurations. An experiment was performed at Sandia National Laboratories using 400kV, 50kA and 50ns beam generator. During experiment planar geometry MILO was considered employing 15 cavities. It was concluded that MILO can be operated in a line-limited

and load-limited conditions for which load is placed at the end of device, allowing independent adjustment of impedance. In 1988, Marder simulated a Magnetically Insulated Line Oscillator using pseudo-current algorithm for parameters optimization. MILO operation also depends on the region of electron emission and on power extraction from the cavities. The main parameters characterizing MILO are: G-anode-cathode gap, D-depth of cavities, S-periodic spacing of vanes, W-width of vanes. The simulations are compared with both linear theory and experimental data. The simulated MILO for 500kV, 50kA with 8 interaction cavities generated an output power of 2.1GW with an overall efficiency of 10.9% at 50ns.

In 1989, Lemke has reported on linear stability of space charge flow in MILO wherein microwaves are generated via unstable interaction between slow electromagnetic modes and space-charge waves. A dispersion relation was derived for transverse magnetic modes in a cylindrical MILO. This was solved numerically to obtain MILO frequency spectrum and instability growth rates. Further simulations work ensured that MILO frequency cannot be changed by varying the applied voltage. In 1995, Ashby *et al.*, have reported an experimental and simulation results of L-band MILO with a number of simple axis-symmetric discs at 1GHz for 500kV, 21kA with an efficiency of 10.8%. In 1997, R. W. Lemke *et al.*, have investigated non-linear regime in a load-limited MILO considering limitations on power conversion efficiency by using numerical simulation. The dc operating characteristics of MILO are determined by a current-carrying load which forms a part of a unique power extraction scheme. The maximum power is obtained when an RF choke is used for the upstream boundary and the maximum efficiency is accomplished by considering the spokes collectively as a modulated dc current crossing a voltage-modulated gap. The PIC Simulation of L-band MILO gave an output power of 3GW for 493kV, 56.2kA with an efficiency of 10.8%.

In 1997, M.D. Haworth *et al.*, demonstrated Hard-Tube (HT) MILO experiment at L-band and obtained 3.2GW for 500kV, 60kA. HTMILO tube is different from the original tube in two respects such as extractor is supported by six quarter wavelength stubs rather than by four stubs making gravity contact with the outer conducting wall. HTMILO has a tapered cathode shank in the choke vane region while the original MILO has a constant radius cathode over the entire length of the tube. By changing to the tapered shank in the choke region allowed the HTMILO to increase its output power.

During 1998 M.D. Haworth *et al.*, have studied significant Pulse Lengthening in a multi-gigawatt MILO. The progress achieved in radiating higher peak power level in HPM source has been hampered by the pulse shortening problem. The design of MILO is an important issue for the present development in the field of high power devices for the different applications. MILO has been taken into consideration by various researchers in order to improve phenomena of pulse shortening and shot-to-shot reproducibility. The main issue in the development of MILO is that it develops poor efficiency. The key operational parameters for a MILO are peak power, efficiency, pulse duration or energy per pulse. Maximizing power and efficiency has been an active area of research taking into consideration various beam and structure parameters. In 1998, Eastwood *et al.*, reported the tapered MILO at L-band for 460kV containing 16 cavities with efficiency of 20-40% and this MILO was designed with novel tapered slow-wave structure and axial power extraction. Two important novel features were introduced by Eastwood into the tapered MILO. The first was the cavity depth taper, which increases the group velocity of the slow-wave structure with axial position. The second was to place the diode into the slow-wave interaction space to allow further energy recovery from the diode current. The taper also leads to an increasing phase

velocity, but the phase focusing and bunching mechanisms in crossed-field flow keeps the electrons in synchronism with the wave to allow extra amplification of the RF signal. The performance of the tapered MILO depends on both the location of the diode and the diode gap. Increasing the number of cavities in the interaction space by moving the diode further down the taper (the direction) increases power and steady-state efficiency, but increases the time taken to reach steady state. The current in the MILO is carried by electron flow across the interaction space from cathode to anode. This current may be divided into two parts: that which flows to the outer anode. Structure and that which flows to the inner cylindrical part of the anode to the right of the diode. The latter part of the current is largely responsible for the insulating magnetic field, while the former part feeds the RF. The simulations results predicted efficiencies up to 20% of tapered MILO.

In 2000, Bao-Liang Qian *et al.*, in 1995 have analysed the relativistic para-potential electron flow in MILO. The distribution expression of the velocity, energy, density and self-electric and self-magnetic fields of electron flow are derived and numerically solved. Yulin yang *et al.*, 2001 reported a novel method for increasing MILO frequency considering the design of a high power and high frequency MILO. In addition to the surface emission on the cathode, the end emission from the cathode is incorporated in order to enhance the self-insulated magnetic field and to reach Hull cut-off criterion. Using a 2-D PIC simulation, an output power of 1.16GW at C band and 270 MW at X band in a MILO have been achieved. In 2001, M.D.Haworth *et al.*, have proposed an improved cathode design for long pulse MILO operation that extended the radiated microwave pulse duration from 200ns to 400ns. This was accomplished by maximizing the emission uniformity in the launch point region of the cathode which in turn reduced the anode plasma formation. Subsequently an improved Electrostatics Design for

cathodes by implementing of miniaturized Pierce focusing electrodes on each end of the MILO cathode as a way to control the beam current density and to minimize anode plasma was reported.

In 2005, Richard Cousin *et al.*, reported the theoretical and experimental behaviour of a compact MILO electromagnetic structure in which all dimensions of US Air force design were reduced by factor of 2. The preliminary simulation of this compact MILO containing 4 interaction cavities using MAGIC PIC- code is studied. The output power of more than 1.0 GW at a frequency of 2.44 GHz for the operating voltage 500 kV, 45kA. Further power output can be increased to 2GW by optimizing the output coupling and reducing the beam loading effect. In 2005, Fan Yu-Wei *et al.*, proposed a compact MILO with new-type of beam dump. The improved MILO consists of a novel beam dump, one cavity RF choke section in place of 2 RF choke section and a novel mode-transducing antenna was simulated using KARAT PIC code. This produced an output power of 2GW for the voltage of 520-540kV and current of 58-62kA. In 2007, Fan Yu-Wei *et al.* reported the simulation investigation of an improved MILO at 1.76GHz for 600kV and 52KA and achieved an output power of 4.2GW with Peak power conversion efficiency of 12%. A novel plate-inserted mode-transducing antenna, comprising a plate-inserted mode converter and a coaxial horn, is introduced into the improved MILO. The *TEM* wave generated by the MILO propagates down the section of coaxial waveguide and is transformed into the TE_{11} mode by the novel plate-inserted mode converter, and then radiated by the coaxial horn antenna into air. The direction of the radiated microwave agrees with the axis of the MILO. In 2006, Zhang Xiao-ping *et al.*, simulated a novel compact P-band MILO at 630 MHz using KARAT PIC code. This produced an output power of 4.7GW with peak power conversion efficiency of 14.9% at 700kV, 45kA. This MILO has one choke vane and 4-interaction cavities.

In 2007, Richard Cousin *et al.*, reported a Gigawatt class of MILO that was driven by a low-impedance Marx generator. The operating frequency of 2.40 GHz is confirmed by measuring the emitted radiation using both an in-vacuum antenna and a horn placed in the far-field region. The frequency response of the MILO was compared with 3-D simulation performed with MAGIC. In the first experiment, a microwave output power of 1 GW was obtained, which is in good agreement with the simulation results. Fan Yu-Wei *et al.*, in 2007 have proposed a double band high power microwave source for increasing the power conversion efficiency of MILO. An axially extracted virtual cathode oscillator (VCO) was introduced to utilize the load current in the MILO. This is called MILO-VCO configuration in which both are synchronised to generate HPM. This was simulated of MILO-VCO using KARAT code and generated an output power of 5.22GW with an efficiency of 16.3%. In this MILO-VCO combination, the peak power of MILO is 3.91GW at 1.76GHz and peak power of VCO is 1.33GW at 3.79GHz. In 2008, Fan Yu-Wei *et al.*, reported complex MILO comprising MILO-1 and MILO-2 for improving the power conversion efficiency. In this configuration MILO-2 is used as a load for MILO-1. The load energy of MILO-1 is utilized to generate HPM in the MILO-2. The simulation complex MILO generated an output power of 4.37GW (MILO-1), 2.82GW (MILO-2) at an operating frequency of 1.76 and 1.78GHz respectively for 620kV, 58.4kA. Thus the power conversion efficiency of complex MILO is 19.9% which is an increase of 50% over the conventional load limited MILO.

Wenyuan Yang in 2008 has proposed a C-band MILO comprising 5 vanes and 4 cavities without choke vane and an impedance discontinuity at the launch point. This MILO was driven by 500kV, 40kA. By tapering the extraction region and adjusting the axial width of first vane, the output efficiency was enhanced to ~11% with an output

power of 2.1GW at 3.72GHz. In 2008, Fan Yu-Wei *et al.*, have investigated an X-band MILO which is hybrid one using a RF choke section as well as a tapered cathode at the upstream boundary of the slow-wave structure. In order to increase the length of the interaction region, a ten-cavity SWS is used in this MILO. The simulated X-band MILO was driven by a 720 kV, 53kA electron beam that comes to a nonlinear steady state in 4.0 ns with an average power of 4.1GW, at 9.3 GHz with power conversion efficiency of 10.8% . This is experimentally validated for the applied voltage of 400 kV and the current of 50 kA with the radiated microwave power about 110MW at 9.7 GHz. Since the surfaces of the cathode end and the beam dump are destroyed, the diode voltage cannot increase continuously. The experimental results are greatly different from the simulation predictions due to cathode flare formation and anode plasma formation. In 2008, Fan Yu-Wei *et al.*, have proposed repetition rate operation of an improved MILO and it was initially tested at 550kV, 54kA from 0.5Hz to 3Hz using velvet based cathode and graphite cathode. The output power of 3.1GW at 1.755GHz was obtained with power conversion efficiency of 10.4%.It was found that the shot to shot reproducibility is very good for graphite cathode as compared to a velvet based cathode .The radiated microwave power is less than 1.0dB during the bursts even when the device is operated at 20Hz repetition rate. In 2009, Li Zhi-Qiang *et al.*, have simulated S-Band Tapered MILO for more microwave power and higher efficiency. The distance between the load support legs and the last vane is greatly affecting the operation characteristics of this device. Further the experimentation of this MILO which generated peak power of 2GW at 2.63 GHz with beam conversion efficiency of 11%.

Jin-Chuan Ju *et al.*, in 2009 have designed an improved X-band MILO that addresses several deficiencies found in earlier experiments. In the new structure, an improved

design of launch point is introduced which improves the E -field uniformity on the cathode surface for suppressing the cathode flare formation. Additionally a new design for the load region is presented in which the end of the cathode consists of four polymer velvet rings, a mesh is adopted as anode of the load and a metal barrel is employed as the beam dump. These improvements reduce energy deposition in the beam dump to less than 30 J/g which probably reduces plasma formation in the load region. This improved MILO produced a peak power of 3.5GW for 690kV, 48kA at 9.26GHz. Fen Qin *et al.*, 2009 proposed a novel four cavity ladder cathode compact MILO in L-band is presented which is more compact and high power conversion efficiency using 2.5D PIC simulation. Employing electron beam of 578kV, 46.5kA, RF power output of 5.1GW with power conversion efficiency of 18.9% was obtained compared to 13.7% of the previous model with same beam voltage. In 2009 Wang Dong *et al.*, have proposed MILO oscillating in a modified HEM_{11} mode as its main interaction mode. The excitation of the oscillation mode is made possible by carefully adjusting the arrangements of each resonant cavity in 2-D slow wave structure. For 441kV, 39.7kA, it generated microwave power of 1.47GW in a modified HEM_{11} at 1.45GHz. The power conversion efficiency is about 8.4% and actually the generated microwave is in a TE_{11} like circularly polarized mode, its polarization is decided by the rotation direction of the SWS. The advantage of HEM_{11} is that it has non zero azimuthal wave number that made easy coupling of TM_{00} between neighbouring cavities. In 2009, Renzhen Xiao *et al.*, have designed high efficiency annular MILO-Transit Time Oscillator(TTO) with three separate frequencies in three bands. TTO is introduced to utilize the load currents of an annular MILO called annular MILO-TTO which consists of inward emitting MILO, outward emitting MILO and coaxial TTO. The simulated responses

showed that the three MILO configuration with 3.2, 9.6, 7.0GW with total efficiency of 25.4% for the input power is 78GW for the beam voltage of 520kV.

Jin-Chuan Ju *et al.*, in 2009, have investigated novel dual-frequency MILO with two separate, stable, and pure HPMs and have taken the concept of L-band MILO. The dual frequency MILO is divided into two MILOs, MILO-1 in C band and MILO-2 in the X-band. The simulated results showed that the three MILO when the dual-frequency MILO is driven by electron beam with 610kV, 82kA, the two HPMs are generated with total power of 5.9GW with power conversion efficiency is about 12%. MILO-1 generated power of 3.2GW at 7.6GHz and MILO-2 at 9.2GHz with output power of 2.7GW. The proposed dual-frequency MILO has got two merits: (i) high efficiency (ii) frequency adjustability. Renzhen Xiao *et al.*, in 2009 have simulated an inward-emitting MILO with 7 tapered cavities at 1.7GHz with an enhanced power conversion efficiency of 19% as compared to a conventional MILO at 1.76GHz is about 12% efficiency. The high efficiency was achieved for 860kV, 74kA. Therefore, the maximum efficiency for inward-emitting MILO is 1.6 times higher than the conventional MILO. The inward emitting MILO is a potential HPM device having single frequency spectrum and higher efficiency. In 2009 Dai-Bing Chen *et al.*, have presented a bi-frequency (BF) MILO with a novel idea of azimuthal partition to generate HPM with the two frequencies of 3.4GHz and 3.65GHz in a single device. This MILO is realized by tuning the cavity-depth of a conventional MILO in azimuthal direction along with self-insulated current, total anode current and total impedance as same as conventional MILO. The simulated C-band BFMILO stably yielded output power of ~1.43GW for 490kV, 45kA with the power conversion efficiency is ~6.5%. The amplitude difference between the two microwaves in the spectrum is about 0.4dB.

Jin Chuan Juet *et al.*, in 2009, have reported an X-band conventional MILO for voltage of 694kV, current of 48.4kA. The simulated MILO generated RF power of 4.1GW at 9.26GHz, with power conversion efficiency of 12.2%. An improved bi-Frequency (BF) MILO was simulated by Dong Wang *et al.*, in 2010 for generating microwave power at 1.21GHz and 1.46GHz using intrinsic field distribution. The high frequency analysis showed that it has a better field distribution than the original one. The improved BF-MILO yielded microwave power of 2GW while the output power is 1.7GW for the original one for the same beam voltage of 445kV and 39.7kA. Renzhen Xiao *et al.*, in 2010 reported high efficiency X-band MILO with a separate cathode for improving microwave characteristics. The separate cathode has three parts with gradually decreased radii which are divided by two deep grooves and only partial cathode surfaces are allowed to emit electrons. This MILO produced an output microwave power of 6.9GW at 9.26GHz with efficiency of 20.6% 706kV, 47.6kA as compared to 12.2% obtained in a conventional cathode X-band MILO.

In 2011 Fen Qin *et al.*, have introduced a novel method to depress higher order mode generation in MILO which is due to asymmetric beam emission or slightly asymmetric structure in MILO device. The excitation of higher order modes was depressed by adjusting the SWS and high power microwave in purified TEM mode was obtained. The simulated MILO oscillated at TM_{00} mode and successfully depressed the higher order mode i.e. HEM_{11} mode. For the beam voltage of 480kV, current of 46kA and TEM mode of microwave with an output power of 734MW at 3.54GHz was generated which in contrast with the original device with TE_{11} mode at 3.68GHz. Fan Yu-Wei *et al.*, have investigated 1.2GHz MILO in 2011 both experimentally and numerically using KARAT code. For the voltage of 680kV and current of 53kA, microwave power of 4.15GW is produced at 1.169GHz with beam conversion efficiency of 11.5%. The

coaxial TEM mode generated by MILO is converted into TE_{11} mode by a mode converting antenna with the gain of 16.3dBi with the aperture efficiency of the conical horn antenna of 79% at 1.169GHz. The 3-dB beam widths are 24° in E-plane and 32° in H-plane and the side lobes of the radiation patterns are both less than -21dB. The experimental MILO was driven by 590kV, 49kA and obtained microwave power of 2.9 ± 0.3 GW at 1.2GHz for the pulse duration of above 20ns with the power conversion efficiency of 10% .

Smrity Dwivedi *et al.*, in 2012 have carried out electromagnetic analysis of a disk loaded co-axial waveguide structure for MILO excited in TM mode. In the analytical model, Mode matching technique has been used along with all the space harmonics generated due to the structures axial periodicity and stationary modal harmonics caused by the reflections from the disk walls in the disk occupied region of the structure. The dispersion and interaction impedance characteristics of the MILO structure were simulated using CST Microwave studio. This study would help in understanding the physics and in selecting the coaxial disk loaded structure parameters for the use in MILO devices having reasonable RF growth rate in synchronism with electron beam. Jie Wen *et al.*, in 2012 have reported a novel MILO having stable frequency and high efficiency which was obtained by slotting plates with 2-D periodic slow wave structure. In this MILO, the symmetrical and low-level asymmetrical modes have the same working frequency which makes the frequency of the microwave stable during modes competition. Simultaneously the efficiency is increased after the beam crosses the gap on the plates. The PIC simulation indicates that HPM with pure frequency of 1.22GHz and multi-modes of TEM, TE_{11} and TE_{21} are generated and the peak power is increased to 2.8GW from 2.4GW compared with original MILO, when the voltage is 450kV and the current of 43kA. The frequency is stable after asymmetrically excited.

In 2012, Heng Zhou *et al.*, have investigated high Impedance MILO with hollow load and proposed methods to increase the MILO impedance and decrease the anode current. A MILO with impedance of 30Ω and power conversion efficiency of 25% was simulated. Compared with previous MILO, the anode current was reduced about 50% and doubles the power conversion efficiency and the power deposition on the anode is reduced nearly one half. The load current is reduced to 4.6kA, only 17% of the total anode current. Finally a hollow load is introduced to reduce the power deposition density on the load without decreasing the power conversion efficiency. For the voltage of 810kV and current of 26.9kA with an impedance of 30Ω , the RF power of 5.5GW at 1.74GHz has been obtained. Fen Qin *et al.*, in 2012 have investigated S-band higher order mode depressed MILO using L-ladder cathode using 3-D code where all dimensions are divided by a factor of 2. Higher order mode depressed MILO was introduced to depress generation of higher order mode in this device. A TEM mode with an output power of 6.2GW at 2.48GHz was generated for the beam voltage of 830kV, current of 62.2kA with the power conversion efficiency of 12%. In 2013 Jie Wen *et al.*, have investigated Ku-band MILO numerically as well as experimentally for the first time. The MILO was optimized using PIC code. Reflect cavities were introduced to reduce the field intensity between cathode and anode. The simulated MILO generated microwave power of 2.48 GW at 12.5 GHz for 478 kV, 48.9 kA. The experimental MILO generated RF power of 89MW for 539 kV, 57 kA at TM_{01} mode for the pulse width of 15 ns.

Dwivedi and Jain in 2013 have optimized and enhanced RF characteristics of the S-band MILO using MAGIC PIC code for 600kV, 35kA. This MILO device was analysed for its designed value of 600 kV, 35 kA and obtained 1.0-GW of RF output power with power conversion efficiency of $\sim 6\%$ for the typical design parameters. The

optimized S-band MILO structure produced the output power of 2 GW. In 2015 Tao Jiang *et al.*, have simulated an improved Ku-band MILO to eliminate the electrode erosion in the load region. Theoretical calculations predicted that both the current density and the energy deposition density of the improved load are much smaller than those of the traditional plane diode load, hence the electrode erosion was greatly reduced. An improved coaxial extractor with a gradient inner conductor was introduced to achieve efficient microwave extraction and a single coaxial TEM output. The simulation results showed that the right amount of microwave reflection generated by the gradient inner conductor which helps in strengthening the oscillation of the resonant cavities and the beam-wave interaction, thus enhancing the microwave output efficiency. The improved Ku-band MILO is optimized numerically using PIC code. The simulated MILO produced an output power of 2.7GW for 450kV, 48kA at 12.5GHz with the power conversion efficiency of ~13%.

Table-1.1 and Table-1.2 shows the improvements in performance of MILO device and Comparison of MILO with the Other HPM devices respectively.

Table-1.2: Improvements in Performance of MILO device.

Parameters Variation	Research Group	Power, Frequency, Voltage, Current and Efficiency	Remarks
Invented by Experimentation	M. C Clark and R.W. Lemke, 1987	2.0GW,1.5GHz, 400kV, 50kA,10%	Experiment
MILO with Ladder cathode	Fen Qin <i>et al.</i> , 2009	5.1GW , L-band, 578kV, 46.5kA, 19%	Simulation
MILO with separate cathode	Renzhen Xiao <i>et al.</i> , 2010	6.9GW, 9.26GHz, 706kV, 47.6 kA, 20.6%	Simulation
Surface emission on the cathode along with the end emission	Yulin Yang <i>et al.</i> , 2001	1.16GW at C-band; 270MW at X-band	Simulation
Tapered cathode shank in the choke-vane region with constant radius cathode over the entire length of the tube	M.D. Haworth <i>et al.</i> ,1997	3.2GW ,1.5GHz, 500kV, 60kA, 10.6%	Simulation
	Jin-Chuan Ju <i>et al.</i> , 2009	3.5GW, 9.26GHz, 690kV,48kA , 10.5%	Simulation

Maximizing the emission uniformity in the launch-point region of the cathode for reducing the anode plasma formation	M.D. Haworth <i>et al.</i> , 2001	L-band	Experiment
Simple axis-symmetric discs	Ashby <i>et al.</i> , 1995	1.1GW, 1GHz, 500kV, 21kA, 10.8%	Simulation
Tapering of SWS vanes for the Tapered MILO	Eastwood <i>et al.</i> , 1998	L-band, 460kV, 20-40%	Simulation
	Li Zhi-Qiang <i>et al.</i> , 2009	2GW , 2.63 GHz, 11%	Simulation
Introduced novel beam dump, one cavity RF choke section in place of 2-cavity RF choke section and a novel mode-transducing antenna	Fan Yu-Wei <i>et al.</i> , 2005	2GW ,1.76GHz, 520-540kV ,58-62kA	Simulation
One choke-vane instead 2 choke-vanes	Zhang Xiao-ping <i>et al.</i> , 2006	4.7GW, 630GHz, 700kV, 45kA, 14.9%	Simulation
One choke vane along with tapered extraction region	Wenyuan Yang, 2008	2.1GW, 3.72GHz, 500kV, 40kA, 11%	Simulation
One choke vane instead of 2 choke with tapered cathode with ten-cavity SWS	Fan Yu-Wei <i>et al.</i> , 2008-1	4.1GW, 9.3 GHz, 720 kV, 53kA, 10.8%	Simulation
	Fan Yu-Wei <i>et al.</i> , 2008-1	110MW, 9.7GHz, 400 kV, 50 kA	Experiment
MILO with Repetition rate operation using Graphite cathode	Fan Yu-Wei <i>et al.</i> , 2008-2	3.1GW ,1.755GHz, 550kV, 54kA, 10.4%	Experiment
Plate inserted mode converter and a coaxial horn	Fan Yu-Wei <i>et al.</i> , 2007	4.2GW, 1.76GHz, 600kV ,52KA, 12%	Simulation

Table-1.3: Comparison of MILO with the other HPM devices

Parameters	MILO	Vircator	Reltron	Relativistic Magnetron	Relativistic BWO	Gyro-devices	Free Electron Laser
Operating Frequency	Upto Ku-band	Upto X-band	Upto X-band	Upto X-band	Upto X-band	mm & sub-mm	mm & sub-mm
Efficiency	20-30%	1 - 3%	30-40%	20-30%	40%	40-50%	40%

External Magnetic field Required or not?	No	No	No; but $\geq 1\text{GW}$, Ext Magnetic field required	Yes	Yes	Yes	Yes
Size	Compact	Compact	Heavy	Heavy	Heavy	Heavy	Heavy
Imp. matching required or not with pulse power supply?	No	No	Yes, Very high impedance	Yes	Yes	Yes	Yes
Osc. or Amp.	Osc.	Osc.	Osc.	Osc.	Osc.	Osc./ Amp.	Osc./ Amp.
Construction complexity	Simple	Simple	Complex	Complex	Simple	Complex	Complex
Oscillation mode	TM_{01}	TM_{0n} modes	TE_{10}	TM_{01}	TM_{01}	TE modes	TEM
Input voltage changes, Frequency oscillation changes?	No	No	No changes, if self mag field Yes, if external magnetic field applied	Yes	Yes	No	No
Repetitive Operation	Upto 20Hz	Single shot	Single shot	Upto 250Hz	Upto 500Hz	Single Shot	Upto 2kHz

1.7. Motivation and Objective

The motivation for research and development of MILO device is led from its strategic applications where it can be potentially used. During the last two decades, MILO has emerged as a HPM device which is simple, compact and efficient high power microwave (HPM) source that are in demand for the latest upcoming applications in E-bomb and Directed Energy Weapons (DEW) systems because of no requirement of the external DC magnetic field. During past and present scenario, significant works, including simulation, theoretical and experiments have been carried out for the performance improvement of MILO. However, presently designing of the MILO, taking into account the pulse shortening problem, shot-to-shot reproducibility remains a critical issue for its developers. This aspect perhaps motivated the author and several other researchers to associate, contribute and enhance the knowledge for this important problem in MILO device. Maximizing the output power, improvement in lifetime of Explosive emission cathode and efficiency are still an active research area worldwide. These performances related issues of the MILO motivated the author to choose the current topic as his doctoral research work. Objective of thesis is to contribute some work related to performance and improvement in beam-wave interaction process in MILO, so that maximum beam power conversion efficiency can be achieved for getting maximum RF power the output. In view of the above, author optimizes design given in literatures and taking into account effect of impedances at input /output end and pulse shortening problem.

1.8. Plan and Scope

The Magnetically Insulated Line Oscillator (MILO) is a crossed-field, compact HPM device that can generate gigawatts of peak power at the microwave frequency range from L-to Ku-band. Here, generation of self magnetic field is an important property of the device due to electron current flow in the circuit so that electrical breakdown between cathode and anode is prevented. Thus, there is no requirement of the external DC magnetic field and the device is able to handle extremely large input power (more than ten's gigawatts) at modest applied voltages (several hundred kilovolts). MILO has emerged out as a relatively new HPM device which is compact, simple, light weight, and high-efficiency capability. This has motivated the author to take up the electromagnetic wave and electron beam interaction study, design, simulation, optimization and experiments in the present thesis. Accordingly, the thesis is divided in seven chapters, as follows.

In Chapter 1, an overview of HPM system and literature survey and status of development of various HPM devices as well as applications are described. Both the relativistic versions of the conventional microwave tubes as well as special plasma vacuum devices are reviewed and found that the MILO device is an attractive HPM source for generating High Power Microwaves. Basic principle, working, advantages, and limitations of the device are briefly explained. A detailed literature review has been carried out for the development of MILO device, present status, issues and limitations as well as different device versions for its performance improvement. Comparison of MILO with the Other HPM devices is explained in detail. The author has brought out the motivation and objective of the thesis. Also performance improvements in MILO device from invention to till date are described. The plan and scope of the present thesis is also outlined in this Chapter 1.

In Chapter 2, the analytical fundamentals of the crossed field device are described threadbare. Under the crossed field devices, there are two types of particle motion, the classical motion and relativistic motion; besides it, different type of emission process like explosive, distributed etc. is also reviewed with fundamentals and basic equations. The condition for explosive emission and magnetic insulation which occurs in MILO device are also presented. Various currents produced by MILO device are described. Using the MILO design methodology presented, the basic design expressions are derived in this Chapter 2.

In chapter 3, design methodology using analytical approaches for MILO is presented. Various numerical techniques, like, FIT, FDM, FEM etc., used for the simulation of MILO are explained. In this chapter S-band MILO is designed using analytical formulations. The region of operation of MILO based on Hull cut-off and Buneman-Hartree condition is arrived at for the designed parameters. Further, equivalent circuit approach for the four cavity RF interaction structure in the absence of electron beam is carried out for getting dispersion characteristics from which pi-mode frequency is obtained and also pi-mode frequency derived from equivalent circuit approach is verified through electromagnetic simulation for a 4-cavity MILO RF interaction structure. Then, the entire S-band MILO device is PIC simulated reconfiguring the commercial 3D PIC code by introducing electron beam for studying about the beam-wave interaction mechanism and for obtaining RF power at the output at fundamental mode. The author is brought out spoke current formation at different instant of time during simulation. Further, parametric optimization is carried out for the enhancement in the overall device efficiency. Enhancements of efficiency due to various parameters and its effects in getting output power from MILO device are described. The MILO simulated results are also benchmarked with the help of the available published data.

In chapter 4, Particle Swarm optimization (PSO) technique is used for the optimization of various parameters of RF interaction structure of S-band MILO device, namely, cathode radius, SWS vane inner radius, circuit periodicity between vanes and thickness of SWS vane. Also, different ANN techniques used for optimization are briefly described. PSO parameters control and Flowchart of PSO for the optimization are explained. Fitness function for PSO and optimization of parameters of RF interaction structure of S-band MILO are discussed. After optimization, the device is simulated in CST particle studio for the optimized Parameters using PSO. Comparison of simulated results after optimization using PSO algorithm and parametric technique are presented. It is observed that the enhancement in the efficiency for the optimized parameters using PSO over the parametric optimization technique.

In chapter-5, beam absent (cold) simulation and characterization of RF interaction structure of S-band MILO is described. Four cavity RF interaction structure is designed using analytical formulations. Then, the structure with both ends having end plates made of metals are simulated with two probes in which one probe act as input coupler and the other probe act as an output coupler. The dispersion characteristics are derived from which pi-mode frequency is obtained. Further, the RF interaction structure is fabricated in MTRDC, DRDO, Bangalore using high precision CNC machines. Cold test measurements using scalar network analyser based on Resonant Perturbation technique are carried out. Dispersion characteristics and pi-mode frequency are obtained from the cold test measurements. The author also explained here about the resonant perturbation technique applied for this measurement. It is observed that the measured pi-mode frequency is to be in close agreement with that obtained from the analysis and simulation.

In Chapter 6, design and simulation for proving the concept of self-magnetic insulation of MILO device is described. The structure has been fabricated using stainless steels material and experiments are carried out with the available pulse power supply (KALI-200) at MTRDC. The concept of self-magnetic field generation in MILO is proved from the experiment. The piece parts and final assembly drawings of MILO device are made using solid works modelling software. Further, the piece parts of S-band MILO have been fabricated at MTRDC. MILO delivers RF power at output in TM_{01} mode where main lobe carries minimum RF power and side lobes carry maximum RF power which is undesirable for many applications. To radiate the RF power from MILO in TE_{11} mode, mode convertor called Vlasov antenna with perspex window have been designed and simulated in CST studio. Later, the parts of Vlasov antenna and window have been fabricated using SST and perspex material, respectively. The MILO device with Vlasov antenna have been integrated with Pulse power supply available at MTRDC, Bangalore and tested for its performance.

Finally, in chapter 7, the work embodied in the present thesis is summarised, and the significant conclusions are drawn from the major findings. The limitations of the present study are also discussed pointing out the scope for further work.